Surface Reconstruction with Feature Preservation based on Graph-cuts

Min Wan, Desheng Wang, and Xue-Cheng Tai

Abstract

A novel and fast surface reconstruction method is proposed aiming to preserve features. The effectiveness of the weighted minimal surface model $E(S)$ is examined in the tetrahedral mesh used in this paper. A variation of the model with curvature $E_c(S)$ is proposed for feature preservation. The straightforward iterative approach is firstly presented as well as its disadvantages. A more efficient and robust method is then proposed for the curvature minimization. The supremum and infimum of minima of $E(S)$ are obtained as two curvature estimations. Two estimations are merged into a new graph, the min-cut of which is a very close approximation to the global minimum of $E_C(S)$. Various examples show the effectiveness and the efficiency.

Index Terms

Graph-cuts, Curvature, Delaunay triangulation, Voronoi Diagram.

1 Introduction

Reconstructing a surface from an unorganized point set has been an important yet challenging problem in computer graphic area for the last two decades. As a significant topic in the reverse engineering, the surface reconstruction attempts to make the unorganized data points to be "perceptible" by machines. In the last two decades, various advances have been made in this area. The common goal of various approaches is to reconstruct the surface as faithful as possible from the data set with some interruptions such as noise, outliers, and non-uniformity.

In the reconstruction problem, sharp features are quite desirable for some specific applications such as computer-aided design (CAD). The sharp features represent the high frequency portion of all information carried by a shape. From the knowledge of signal sampling principle, a higher frequency needs a denser sampling, which is hardly met in the practice. For instance, the edges and corners of a cube require infinite sampling to meet the ϵ-sampling [1]. Due to the relatively sparse sampling on the feature, existing reconstruction methods are not able to obtain a result with precise features even under noise free assumption. The demand of a surface reconstruction method with feature preservation motivates this study.

Generally speaking, existing surface reconstruction methods could be classified into two categories, explicit and implicit. Explicit methods are mostly local geometric approaches based on the Delaunay triangulation and dual Voronoi diagram. Typical methods include the

- *M. Wan, D. Wang, X.-C. Tai are with the Division of Mathematical Sciences, School of Physical and Mathematical Sciences, Nanyang Technological University, Singapore 637371.*
  E-mail: wanm0003@e.ntu.edu.sg, {desheng,xctai}@ntu.edu.sg
- *X.-C. Tai is with the Department of Mathematics, University of Bergen, Johaness Brunsgate 12, 5007 Norway.*
  E-mail: tai@math.uib.no

Alpha shape in [2] and CRUST algorithm in [1], and their variations [3]–[5]. One advantage of these methods are their theoretical guarantee. The theorem states that if the point set satisfies the ϵ-sampling, the restricted Delaunay triangulation of the input data set with respect to the surface is homeomorphic to the surface. However, as we mentioned above, such ϵ-sampling could not be met at the sharp features. Besides explicit approaches are subject to a lot of reconstruction difficulties such as noises and outliers.

The other category, i.e. implicit methods, reconstructs surfaces through implicit functions. One important representative is the level set formulation [6]–[15]. The surface is reconstructed as a certain level set in a volumetrical discretized domain. Usually a variational model is introduced. The reconstruction problem is then translated to an minimization problem. With the representation flexibility and mathematical facilities brought by the implicit formulation, the implicit methods are well received among researchers. Graph-cuts have been proven an efficient minimization tool [14], [23]–[28]. By controlling the curvature term in the energy functional as well as in the minimization procedure, some researchers made advances in feature preservation. [9], [16]–[22]. However, to reconstruct surfaces with feature, existing implicit methods are not suitable due to their discretizing schemes. Most implicit methods use grid, regular or adaptive, to discretize the domain. In this case, the precise data points are represented by the grids. To reconstruct precise features under the grid framework is impossible. In this article, one variational surface reconstruction method with feature preservation is proposed based on Delaunay triangulation, implicit formulation, and graph-cuts.

In the proposed method, a tetrahedral mesh is used instead of the grids to avoid the information loss during the discretization. The position information conveyed by the input data is well preserved in the Delaunay based mesh framework. The reconstructed surface is a triangular mesh connecting the input data. This makes the precise feature preservation possible. We also give the theoretical guarantee that a triangular two manifold homeomorphic to the original surface exists in this mesh. We propose a novel variational model for feature preservation. A curvature term and the weighted minimal surface term constitute the energy functional. This energy functional was approached by iteratively local swapping method in our previous study [29]. Iterative local swaps were performed on the neighborhood of the surface to evolve the surface to the global minimum. That method has some disadvantages such as efficiency and robustness. In this study, we propose a more efficient and robust global approach to minimize the energy involving curvature.

We investigate the possible multiple minima for the weighted minimal surface model. If these minimal surfaces are ordered according to the volumes they enclose, two specific surfaces, i.e. the supremum and infimum, carry partial features of the original surface. These two surfaces are proved to be unique and able to obtain via graph techniques. The curvature information of these two surfaces is then merged reasonably into a new graph, the min-cut of which carries most features. The workload to recover the remaining features is much smaller compared with the previous iterative approach.

The remainder of this paper is organized as follows. In Section 2, the tetrahedral mesh generation and the variational model is presented. The theoretical guarantee is also provided. Section 3 presents the iterative local swap to minimize the curvature energy as well as its disadvantages. Section 4 proposes a more efficient and robust method. A global approach consisting of three graph-cuts gives a close approximation to the solution. The flowchart of the whole algorithm is explained. In Section 5, various examples are presented to demonstrate effectiveness and robustness of the proposed method. At last, Section 6 concludes this article.

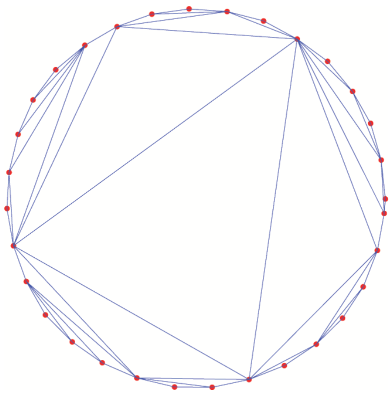

(a) $\mathbf{Del}P$

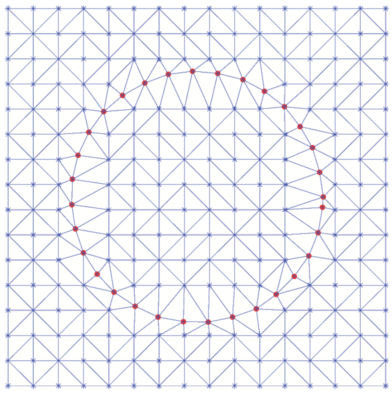

(b) $\mathbf{Del}(P \cup Q)$

Fig. 1. Two meshes with the homeomorphic sub-complex.

2 Tetrahedral Mesh and Variational Model

Let P be a point set sampled from Σ in the domain Ω. The distance from one point to a set is defined as $d(x,Y) = inf_{y \in Y} d(x,y)$, where $d(x,y)$ is the Euclidean distance between x and y. The medial axis M of a surface Σ is the closure of the set of the points that have at least two closest points in Σ. Feature size for a point $x \in \Sigma$ is defined as $f(x) = d(x,M)$. The feature function has the Lipschitz Continuity property, i.e. $f(x) - f(y) < d(x,y)$ for any two points on surface. If for each point $x \in \Sigma$, $d(x,P) \leq \epsilon f(x)$, then the sample P is a ϵ-sample [1]. Amenta and Bern found that a sub-complex, i.e. the restricted Delaunay triangulation of P with respect to Σ, is homeomorphic to Σ for sufficient small ϵ. We cite the theorem as follows:

Theorem 1
Let P be an ϵ-sample of a smooth surface Σ. For $\epsilon \leq 0.18$, the underlying space of $\mathbf{Del}P|_\Sigma$ is homeomorphic to Σ. [1]

2.1 Tetrahedral mesh

Theorem 1 is the theoretical guarantee for most explicit methods. $\mathbf{Del}P|_\Sigma$ is the goal for those methods as illustrated in Figure 1(a). However, in order to apply variational methods and numerical solvers, the mesh formed by only $\mathbf{Del}P|_\Sigma$ is not a reasonable discretization. Usually we need some auxiliary points such as shown in Figure 1(b). In this article, these auxiliary points are called non-geometric points to be distinguished from the input "geometric" data points P. These non-geometric points are denoted as Q.

We hope the homeomorphic sub-complex in Theorem 1 still exists in the mesh consisting of P and Q. Next we prove that there still exists the homeomorphic sub-complex in $\mathbf{Del}(P \cup Q)$ as long as Q is away enough from P.

First, the following Lemma shows that under the ϵ-sample assumption, the sizes of 1- and 2-dimensional faces in $\mathbf{Del}P|_\Sigma$ are relatively small. Upper bound is provided with respect to feature size.

Lemma 1
For $\epsilon < 1$,
(1) The length of an edge pq in $\mathbf{Del}P|_\Sigma$ is at most $\frac{2\epsilon}{1-\epsilon} f(p)$;
(2) The circumradius of an triangle pqr in $\mathbf{Del}P|_\Sigma$ is at most $\frac{\epsilon}{1-\epsilon} f(p)$

Proof:

For any point x in the restricted Voronoi cell $V_p|_\Sigma$, from the ϵ-sample definition, we have

$$d(x,p) \leq \epsilon f(x) \tag{1}$$

From the Lipschitz Continuity, we have

$$f(x) - f(p) \leq d(x,p) \tag{2}$$

Combined the above two inequalities,

$$\begin{aligned} f(x) - f(p) &\leq \epsilon f(x) & (3)\\ f(x) &\leq \frac{1}{1-\epsilon} f(p) & (4)\\ d(x,p) &\leq \frac{\epsilon}{1-\epsilon} f(p) & (5)\end{aligned}$$

For an edge pq in $\mathbf{Del}P|_\Sigma$, which means $V_p|_\Sigma \cap V_q|_\Sigma \neq \emptyset$. Choose one point $x \in V_p|_\Sigma \cap V_q|_\Sigma$, we have both $d(x,p) \leq \frac{\epsilon}{1-\epsilon} f(p)$ and $d(x,q) \leq \frac{\epsilon}{1-\epsilon} f(p)$. By triangle inequality, $d(p,q) \leq d(x,p) + d(x,q) \leq \frac{2\epsilon}{1-\epsilon} f(p)$.

For a triangle pqr in $\mathbf{Del}P|_\Sigma$, which means $V_p|_\Sigma \cap V_q|_\Sigma \cap V_r|_\Sigma \neq \emptyset$. For a point $x \in V_p|_\Sigma \cap V_q|_\Sigma \cap V_r|_\Sigma$ and the circumcenter c of pqr, we have $d(c,p) \leq d(x,p) \leq \frac{\epsilon}{1-\epsilon} f(p)$. □

Since the 1- and 2-faces in $\mathbf{Del}P|_\Sigma$ are small, the insertion of Q would not destroy these faces if Q are away enough from P. We give the following theorem.

Theorem 2

Let P be an ϵ-sample of a smooth surface Σ and Q be the non-geometric points. If for each point $m \in Q$ and $p \in P$, $d(m,p) > \frac{2\epsilon}{1-\epsilon} f(p)$, and $\epsilon \leq 0.18$, the underlying space of $\mathbf{Del}(P \cup Q)|_\Sigma$ is homeomorphic to Σ.

Proof:

1) For an edge pq in $\mathbf{Del}P|_\Sigma$ and any $m \in Q$, we are given: $d(m,p) > \frac{2\epsilon}{1-\epsilon} f(p)$. Combined with Lemma 1,

$$d(m,p) > \frac{2\epsilon}{1-\epsilon} f(p) \geq d(p,q) \tag{6}$$

m resides out of $B_{p,d(p,q)}$, the ball centered at p with radius $d(p,q)$. The circumsphere of edge pq, $B_{\frac{p+q}{2},\frac{d(p,q)}{2}}$, is a subset of $B_{p,d(p,q)}$ as illustrated in Figure 2(a). The fact $m \notin B_{\frac{p+q}{2},\frac{d(p,q)}{2}}$ implies that the insertion of m does not violate the empty sphere property of Delaunay triangulation. pq is still an edge in the Delaunay triangulation of $\mathbf{Del}P \cup \{m\}$.

2) For a triangle pqr in $\mathbf{Del}P|_\Sigma$ and any $m \in Q$, suppose the circumsphere of pqr is $B_{c,rad}$. Lemma 1 states that $rad \leq \frac{\epsilon}{1-\epsilon} f(p)$. We are given $d(m,p) > \frac{2\epsilon}{1-\epsilon} f(p)$. We have:

$$d(m,p) > \frac{2\epsilon}{1-\epsilon} f(p) \geq 2rad \tag{7}$$

The distance between any two points in a sphere is at most the diameter of the sphere. Hence the above inequality shows that $m \notin B_{c,rad}$. According to the Delaunay triangulation property, pqr is still a triangle in the Delaunay triangulation of $\mathbf{Del}P \cup \{m\}$.

Part (1) and (2) shows that all edges and triangles in $\mathbf{Del}P|_\Sigma$ are kept in $\mathbf{Del}P \cup \{m\}$. By incremental inserting all points in Q, all edges and triangles in $\mathbf{Del}P|_\Sigma$ are kept in $\mathbf{Del}(P \cup Q)$, which is equivalent to $\mathbf{Del}P|_\Sigma \subset \mathbf{Del}(P \cup Q)$.

Next we show that $\mathbf{Del}P|_\Sigma = \mathbf{Del}P \cup Q|_\Sigma$. Suppose that for any $p \in P$ and $m \in Q$, such that $V_p|_\Sigma \cap V_m|_\Sigma \neq \emptyset$. Pick any point $x \in V_p|_\Sigma \cap V_m|_\Sigma$. According to the Voronoi cell definition, $d(x,p) = d(x,m)$.

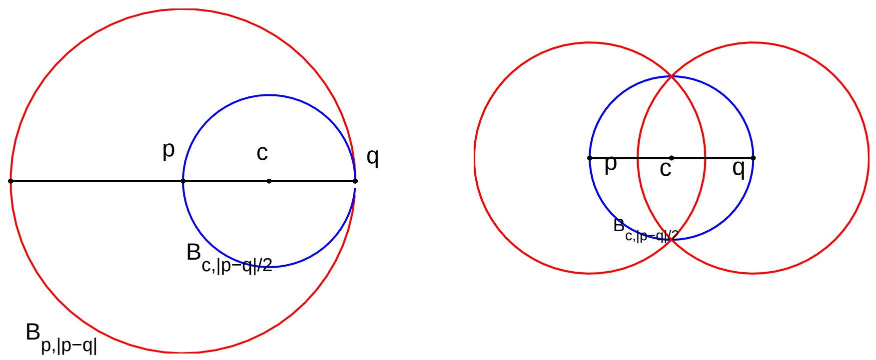

(a) $B_{\frac{p+q}{2},\frac{d(p,q)}{2}} \subset B_{p,d(p,q)}$ (b) $B_{\frac{p+q}{2},\frac{d(p,q)}{2}} \subset B_{p,\frac{\sqrt{2}d(p,q)}{2}} \cup B_{q,\frac{\sqrt{2}d(p,q)}{2}}$.

Fig. 2. Two illustrations showing that insertion of non-geometric points would not destroy S_Σ.

Given by condition, we have

$$d(m,p) \leq d(x,m) + d(x,p) = 2d(x,p) \leq 2\epsilon f(p) \tag{8}$$

The given condition $d(m,p) > \frac{2\epsilon}{1-\epsilon} f(p)$ and above inequality leads to contradiction. Hence $V_p|_\Sigma \cap V_m|_\Sigma = \emptyset$ for any $p \in P$ and $m \in Q$. As the dual to restricted Voronoi diagram, pm is not an edge in $\mathbf{Del}(P \cup Q)|_\Sigma$ for any $p \in P$ and $m \in Q$. Hence $\mathbf{Del}P|_\Sigma = \mathbf{Del}(P \cup Q)|_\Sigma$. Recall Theorem 1 states that $\mathbf{Del}P|_\Sigma$ is homeomorphic to Σ. We can draw the conclusion $\mathbf{Del}(P \cup Q)|_\Sigma$ is homeomorphic to Σ. For the rest of this paper, we assume P and Q satisfy this criterion and denote both $\mathbf{Del}P|_\Sigma$ and $\mathbf{Del}(P \cup Q)|_\Sigma$ by S_Σ.

□

Remark 1
In two dimensional cases, the criterion $d(m,p) > \frac{2\epsilon}{1-\epsilon} f(p)$ in Theorem 2 can be loosened to $d(m,p) > \frac{\sqrt{2}\epsilon}{1-\epsilon} f(p)$. As illustrated in Figure 2(b), the circumsphere $B_{\frac{p+q}{2},\frac{d(p,q)}{2}}$ is subset of $B_{p,\frac{\sqrt{2}d(p,q)}{2}} \cup B_{q,\frac{\sqrt{2}d(p,q)}{2}}$.

In practice, regular grids or body-centered cubic (BCC) lattices could be generated as the candidates for Q. The candidate points are filtered according to the distance to P. The distance criterion proposed in Theorem 2 is with regard to the feature function $f(p)$, which is unavailable. Hence, we need to convert this criterion to a practicable one.

To convert this criterion, certain assumption of sampling uniformity should be made firstly. Usually two uniformity definitions are used, global and local. Since the global uniformity is more restrictive, it is sometimes not met in real cases. We use the local uniformity as our assumption. P, a sample of Σ is locally (ϵ, δ)-uniform for $\delta > 1 > \epsilon > 0$ if each point $x \in \Sigma$ has a point in P within $\epsilon f(x)$ distance and no point $p \in P$ has another point $q \in P$ within $\frac{\epsilon}{\delta} f(p)$ distance [30].

Given a sample P conforming this uniformity assumption, the distance criterion could be revised as follows. First, the Delaunay triangulation of P is generated. For each vertex $p \in P$, the shortest edge incident to p is found and the length is denoted by $h(p)$.

In earlier study, it was shown that the shortest edge incident to p is a Delaunay edge in S_Σ under the ϵ-sample assumption. With the locally uniform assumption, we have $h(p) > \frac{\epsilon}{\delta} f(p)$. For a non-geometric point $m \in Q$, if $d(m,p) > \frac{2\delta}{1-\epsilon} h(p)$, then $d(m,p) > \frac{2\delta}{1-\epsilon} h(p) > \frac{2\epsilon}{1-\epsilon} f(p)$, which is the criterion in Theorem 1. Therefore, the unknown $f(p)$ is replaced by the explicit $h(p)$. And the lattice points can be filtered by this new criterion and obtain Q. The Delaunay triangulation of $P \cup Q$ is generated as the mesh framework denoted by $\mathcal{T}$.

2.2 Variational model

With respect to the reconstructed surface S, the weighted minimal surface model was proposed by Zhao et al. in [8].

$$E(S) = \int_S d(x, P) ds. \tag{9}$$

The watertight surface S is equivalent to a segmentation of domain Ω. In discrete mesh framework $\mathcal{T}$, it is also equivalent to a two-labeling of all elements in $\mathcal{T}$, 1 for interior and 0 for exterior. The labeling for the element K_i is denoted by $l_i \in \{1, 2\}$.

The discrete surface could be represented as

$$S = \bigcup_{l_i \neq l_j} (K_i \cap K_j) \tag{10}$$

The discrete energy functional

$$\begin{aligned} E(S) &= \int_S d(x, P) ds && (11)\\ &= \sum_{i \neq j} \int_{K_i \cap K_j} d(x, P) \mathbf{1}_{\{l_i \neq l_j\}} ds && (12)\\ &= \sum_{i \neq j} d_{i,j} s_{i,j} \mathbf{1}_{\{l_i \neq l_j\}}\,, && (13) \end{aligned}$$

where

$$d_{i,j} = \frac{\int_{K_i \cap K_j} d(x, P) ds}{\int_{K_i \cap K_j} ds} \quad , \quad s_{i,j} = \int_{K_i \cap K_j} ds \tag{14}$$

and the indicator function $\mathbf{1}_{\{.\}}$ is 1 when the statement in brackets is true and 0 otherwise. $d(x, P)$ is piecewise linear on the triangulated two manifold. Hence, $d_{i,j}$ could be approximated as the mean of $d(x, P)$ on the three vertices.

Graph-cuts, as a fast global minimization tool, can be used to approach this energy. A graph $\mathcal{G}$ is built dual to the mesh $\mathcal{T}$. For each tetrahedral K_i in $\mathcal{T}$, a node n_i is added to $\mathcal{G}$. For each triangle face $K_i \cap K_j$ in $\mathcal{T}$, an edge (n_i, n_j) is added to connect n_i and n_j. The cost of edge $cost(n_i, n_j) = d_{i,j} s_{i,j}$. The primal-dual relationship also applies to the segmentation and cut. A surface S segmenting $\mathcal{T}$ corresponds to a cut $\mathcal{C}$ in $\mathcal{G}$. The cost of $\mathcal{C}$ is equal to $E(S)$. Hence finding the min-cut is equivalent to minimizing the energy $E(S_T)$. Next we show that S_Σ corresponds to a min-cut in $\mathcal{G}$.

Theorem 3
S_Σ corresponds to a minimal cut of $\mathcal{G}$.

Proof:

$$E(S_\Sigma) = \sum_{i \neq j} d_{i,j} s_{i,j} \mathbf{1}_{\{l_i \neq l_j\}} \tag{15}$$

where $\bigcup_{l_i \neq l_j} (K_i \cap K_j) = S_\Sigma$.

For each triangle $T_{i,j} = K_i \cap K_j$, $l_i \neq l_j$, we have $T_{i,j} \subset S_\Sigma = \mathbf{Del}P|_\Sigma$. The fact that $T_{i,j} \subset \mathbf{Del}P|_\Sigma$ implies that for all three vertices u, v, w on triangle $T_{i,j}$, $u, v, w \in P$.

$$d_{i,j} = \frac{1}{3}(d(u, P) + d(v, P) + d(w, P)) = 0 \tag{16}$$

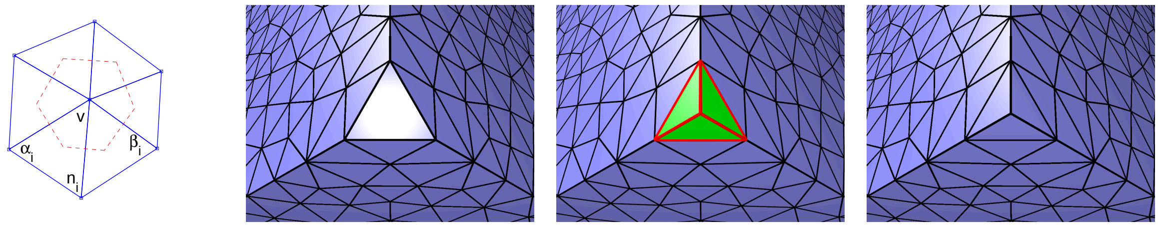

(a) Mean curvature on a triangulated mesh (b) Before the swap (c) Evaluate the swap (d) After the swap

Fig. 3. Illustrations on local swap and energy computation on triangulated two manifold

Thus $E(S_\Sigma) = 0$, the corresponding cut of $\mathcal{G}$ is also zero and hence is a min-cut of $\mathcal{G}$. □

Theorem 3 shows that the weighted minimal surface model could well reconstruct the surface in tetrahedral meshes by graph-cuts. If S_Σ is the unique minimal cut of $\mathcal{G}$, the graph-cuts could obtain the desirable solution. However the minimal is not unique for $E(S)$ in most cases. In order to eliminate this ill-posedness, a revising regularization term is usually added to the model $E(S)$. The regularization with regard to surface area is the most common choice [31], [32].

$$E_A(S) = \int_S d(x,P)ds + \alpha \int_S ds \tag{17}$$

In this case, the graph-cuts approach is still effective if the n-link costs are updated with $(d_{i,j} + \alpha)s_{i,j}$. However, area regularization could not preserve features effectively. The smoothed features are commonly observed in earlier studies. In this paper, we propose a variational model with the curvature regularization term.

$$E_C(S) = \int_S d(x,P)ds + \mu \int_S |\kappa(x)|^2 \, ds\,, \tag{18}$$

where $\kappa(x)$ is the mean curvature of x.

3 Local Approach for Curvature Minimization

The effectiveness of the curvature term in preserving features has been approved by some researchers in other frameworks such as grids [9]. In this paper, the grid is replaced by the tetrahedral mesh. The minimization of any energy functional involving curvature is a more difficult task in a tetrahedral mesh than in grids.

The fast solver, graph-cuts, could be used to minimize the energy only if the high order geometric characteristic could be well transferred to a graph representable term. In the previous study, we proposed a two stage method to tackle this high order issue. Local swaps on single elements are performed iteratively to approach a local minimum of $E_C(S)$. The criterion of swap is a decreasing energy $E_C(S)$ after swap.

Though the curvature is defined on smooth surface, the mean curvature could still be calculated on any triangulated surface mesh [33]. Given a triangulated two manifold Σ_h and a vertex $v \in \Sigma_h$, the one ring neighborhood of v is N_v. With regard to Figure 3(a), the mean curvature of v could be calculated as follows. A normal vector function $\mathbf{K}(x)$ is introduced.

$$\mathbf{K}(x) = \frac{1}{2\mathcal{A}_v} \sum_{\mathbf{n_i} \in N_v} (\cot\alpha_i + \cot\beta_i)(\mathbf{v} - \mathbf{n_i})\,, \tag{19}$$

where $\mathcal{A}_v$ is the Voronoi cell of v restricted to Σ_h. The mean curvature $\kappa(x) = \frac{1}{2}\|\mathbf{K}(x)\|$.

For each triangle $T_{i,j} = K_i \cap K_j$, $l_i \neq l_j$, $\kappa_{i,j}$ could be calculated similar to (16):

$$\kappa_{i,j} = \frac{1}{3} \sum_{u \in T_{i,j}} |\kappa(u)|^2 \ . \tag{20}$$

The method in (19) from [33] is the most "economical" way to estimate curvature on a triangulated two-manifold. Only 1-ring neighborhood is utilized to calculate curvature. Though the optimality and convergence have been shown in [33] and [34] respectively, the accuracy of this approximation is largely dependent on the mesh density as well. In some cases, sparse mesh representation on the high curvature places could not approximate the actual curvature closely enough. Alternatively, some more accurate curvature estimations could be obtained by dilating the region of interest to N-ring neighborhood. All vertices in the dilated neighborhood is utilized in a quadric fitting procedure [35]–[37]. All the first and second fundamental forms could be expressed by the coefficients of the quadric surface. The compromise between the extra computational workload and the relatively accurate curvature must be made. In practice, the cases when (19) is not satisfyingly accurate do occur, however, not often. This quadric fitting curvature approximation method is provided as an alternative way. A hybrid curvature approximation scheme is also under study, which shall be efficient and accurate.

One swap on a single element is illustrated in Figure 3(b)-3(d). Several steps in these iterations on a two-cube example are shown in Figure 4. However, the iterative minimization by single swap has several disadvantages. (a) Efficiency. The iteration is performed on every element adjacent to the surface. The method is quite time-consuming in practice. (b) Local Minima. The greatest problem for any curve/surface evolving method is the local minima traps. The minimization procedure is quite likely be stuck in a local minimum far away from the global minimum. In our reconstruction method, the local minima trap is also a big problem. Extra measures must be taken to help the procedure out of the local minima. Random perturbation similar to simulated annealing may be applied. Sometimes local swaps for single element is not able to recover the features. In this case, the swap object has to be extended to a clique formed by two elements or more. The iteration with respect to all cliques shall be performed after the single element iteration. The combination and priority of various iterations is complicated and heuristic.

4 GLOBAL APPROACH FOR CURVATURE MINIMIZATION

In this section, we propose a more efficient and robust method. In order to approach $E_C(S)$, we investigate the multiple minima of $E(S)$ and its relationship with the variations. Further more, two more models will be introduced to identify some specific minima which convey useful information concerning curvature.

4.1 Multiple Minima

As we mentioned above, $E(S)$ may have multiple minima if discretized in $\mathcal{T}$. It is easy to show that given small enough α and β, the minima of $E_C(S)$ and $E_A(S)$ are also minima of $E(S)$. (The proof is similar to that of Theorem 4) Furthermore, we investigate all minima of $E(S)$.

Suppose we have M minima for $E(S)$ and denote them by $\{S_i\}_{i=1}^{M}$. From Theorem 3, we know that S_Σ is a minimum for $E(S)$ and $E(S_\Sigma) = 0$. It derives that $E(S_i) = 0$ and S_i are all sub-complexes consisting of P. We define that $S_i \leq S_j$ if S_i is enclosed by S_j. Given this order definition, $\{S_i\}$ is a partially ordered set. Then we denote the supremum and infimum

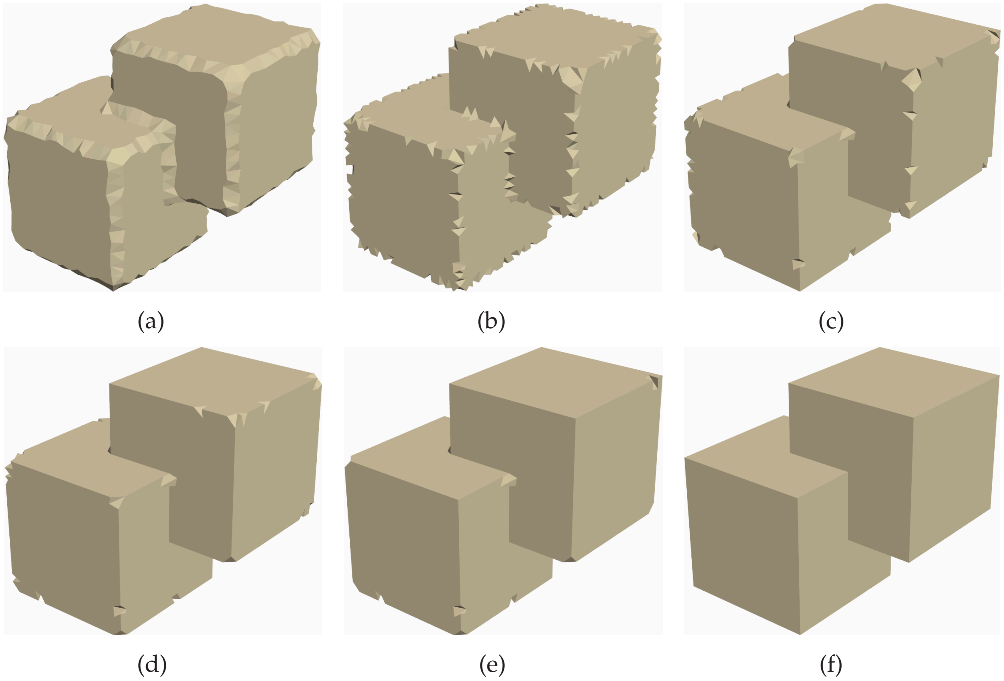

Fig. 4. Several step results in iterations

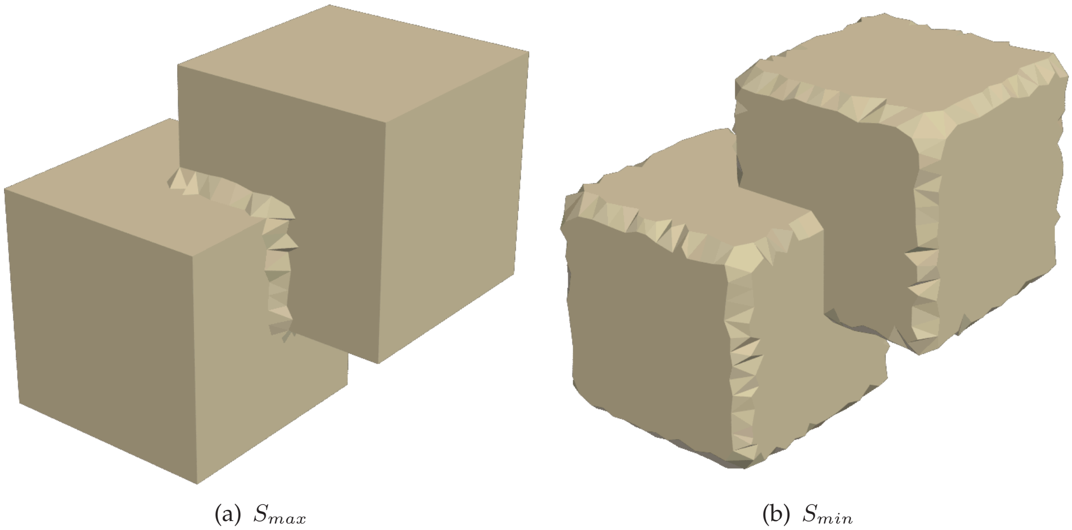

Fig. 5. Supremum and infimum of $\{S_i\}$

of $\{S_i\}$ by S_{max} and S_{min} respectively. Due to the fact that S_i are discrete sub-complex of the tetrahedral mesh, we have $S_{max}, S_{min} \in \{S_i\}$.

We find that S_{max} and S_{min} carry most of features in Σ. Take the two cubes as example, S_{max} and S_{min} are shown in Figure 5. It can be observed that most of features are contained mutually exclusively in these two surfaces. To be more specific, the convex features are included in S_{max} and the concave ones in S_{min}. This discovery gives an hint that these two bounds of $\{S_i\}$ could be used to approach the curvature model $E_C(S)$.

S_{max} and S_{min} are defined as the supremum and infimum of $\{S_i\}$. However, it is not practicable to find them by comparing each pair in $\{S_i\}$. As an alternative approach, we propose two variational models.

$$E_{V+}(S) = \int_S d(x,P)ds + \beta \int_{\Omega_S} d\mathbf{x} \tag{21}$$

$$E_{V-}(S) = \int_S d(x,P)ds - \beta \int_{\Omega_S} d\mathbf{x} \tag{22}$$

where Ω_S is the region enclosed by S. Next we show that the minimum of $E_{V+}(S)$ is S_{min} and the minimum of $E_{V-}(S)$ is S_{max} given small enough β.

Theorem 4
In the mesh $\mathcal{T}$, given small enough β,
(1) The minimum of $E_{V+}(S)$ is S_{min}
(2) The minimum of $E_{V-}(S)$ is S_{max}

Proof:
Denote the minimum of $E_{V+}(S)$ and $E_{V-}(S)$ by S_+ and S_- respectively. Assume τ is the smallest 2-face in $\mathcal{T}$ and s_τ is the area. h is the infimum of $f(p)$, $p \in P$. We know that in mesh $\mathcal{T}$, $E_{V+}(S)$ can be discretized as

$$E_{V+}(S) = \sum_{i \neq j} d_{i,j} s_{i,j} \mathbf{1}_{\{l_i \neq l_j\}} + \beta \sum_i Volume(K_i) \mathbf{1}_{\{l_i = 1\}} \tag{23}$$

Suppose that S_+, is not a sub-complex consisting of P, i.e. $S' \notin \{S_i\}$. There exists at least one vertex $v \in S_+$ such that $v \notin P$

$$\begin{aligned}
E_{V+}(S_+) &= \sum_{i \neq j} d_{i,j} s_{i,j} \mathit{1}_{\{l_i \neq l_j\}} + \beta \sum_i Volume(K_i) \mathbf{1}_{\{l_i = 1\}} \\
&> \frac{1}{3}(d(v,P) + d(u,P) + d(w,P)) \cdot s_{vuw} \qquad \text{(consider only } \triangle vuw,\ v \notin P) \\
&> \frac{1}{3} \cdot \frac{2\epsilon h}{1-\epsilon} \cdot s_\tau \qquad \left(d(v,P) < \frac{2\epsilon}{1-\epsilon} h, \text{ see Theorem 2; } s_{vuw} < s_\tau \right)
\end{aligned} \tag{24}$$

For any $S_0 \in \{S_i\}$,

$$\begin{aligned}
E_{V+}(S_0) &= \sum_{i \neq j} d_{i,j} s_{i,j} \mathit{1}_{\{l_i \neq l_j\}} + \beta \sum_i Volume(K_i) \mathbf{1}_{\{l_i = 1\}} \\
&= \beta \sum_i Volume(K_i) \mathbf{1}_{\{l_i = 1\}} \qquad \left(E(S_0) = \sum_{i \neq j} d_{i,j} s_{i,j} \mathit{1}_{\{l_i \neq l_j\}} = 0 \right) \\
&\leq \beta \sum_i Volume(K_i) \\
&= \beta \cdot Volume(\Omega)
\end{aligned} \tag{25}$$

Combining the above two inequalities, if $\beta \leq \frac{1}{3Volume(\Omega)} \cdot \frac{2\epsilon h}{1-\epsilon} \cdot s_\tau$, (24) (25) could lead to $E_{V+}(S_+) > E_{V+}(S_0)$, which contradict to the fact that S_+ is the minimum. Recall our assumption, it derives that $S_+ \in \{S_i\}$.

For each $S_i \in \{S_i\}$,

$$E_{V+}(S_i) = \beta \sum_i Volume(K_i) \mathbf{1}_{\{l_i = 1\}} = \beta \cdot Volume(\Omega_{S_i})$$

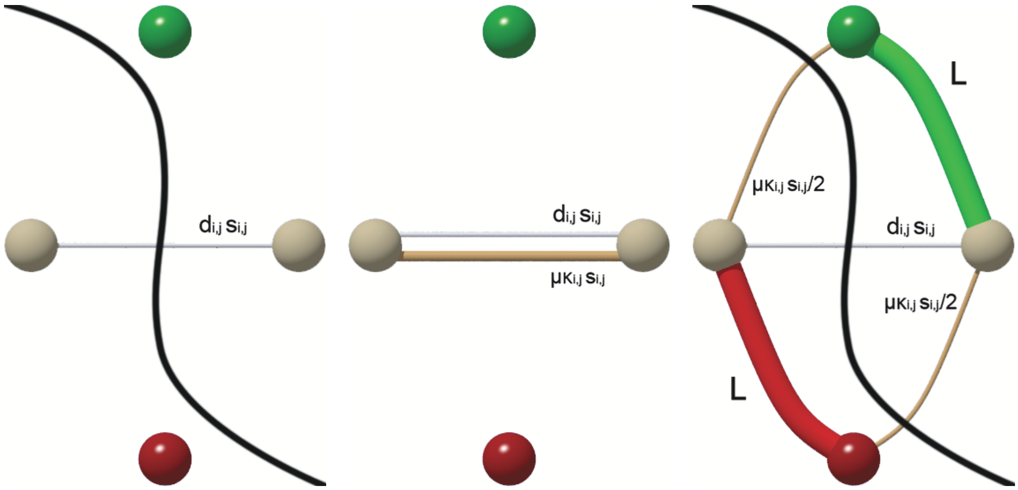

(a) Cut for $E_{V+}(S)$ (b) Compute $\kappa_{i,j}$ explicitly for $E_C(S)$ (c) Redistribute the edge costs for $E_C(S)$

Fig. 6. Process of building a new graph

S_{min} is defined as the infimum of $\{S_i\}$, i.e. $Volume(\Omega_{S_{min}}) \leq Volume(\Omega_{S_i})$ for any S_i. Combining the above identity, we have S_{min} is minimum of E_{V+} for the set $\{S_i\}$. With the fact $S_+ \in \{S_i\}$, we have $S_+ = S_{min}$. Similar proof applies to $E_{V\_}(S)$ as well. $\square$

As shown above, S_{min} and S_{max} are a minimum of $E_{V+}(S)$ and $E_{V-}(S)$ respectively. The uniqueness of S_{min} and S_{max} is trivial. Therefore, minimizing $E_{V+}(S)$ and $E_{V-}(S)$ is well-posed problems and solutions are S_{min} and S_{max}. The graph minimization tool could be utilized on $E_{V+}(S)$ and $E_{V-}(S)$ as well. n-links for (n_i, n_j) are still $d_{i,j}s_{i,j}$. A t-link with cost $\beta Volume(K_i)$ is added to (s, n_i) or (n_i, t). Min-cuts for the modified graph correspond to S_{min} and S_{max}. Next we discuss how to use S_{min} and S_{max} to minimizing $E_C(S)$.

4.2 Graph Approach

Consider a simple case first. The graph $\mathcal{G}$ consists of only two nodes, n_i and n_j. Solving E_{V+} obtains the cut $\mathcal{C}_+$ as in Figure 6(a). Assume $\mathcal{C}_+$ corresponds to the ground truth surface and carries all features. Hence the correct curvature could be calculated explicitly by (19). The curvature term $\mu\kappa_{i,j}s_{i,j}$ for edge (n_i, n_j) is added to $\mathcal{G}$. The $E_C(S)$ could be graph-represented as shown in Figure 6(b). However, the curvature term $\mu\kappa_{i,j}s_{i,j}$ on the n-link has no "sign". $\mathcal{C}_+$ in Figure 6(a) has distinguish the exterior and interior already. It shall be better that the "sign" is utilized as well. Hence the n-link $\mu\kappa_{i,j}s_{i,j}$ is split into two t-links connecting s and t. Meanwhile two large cost t-links are added to the opposite terminals respectively. The modified graph is shown in Figure 6(c). This new graph could guarantee the min-cut is topologically identical to the one in Figure 6(a).

Based on this "split n-link into two t-links" principle, we propose the algorithm in Table 1. Notice that at the end of the algorithm, n-links of $d_{i,j}s_{i,j}$ are updated with $(d_{i,j}+\alpha)s_{i,j}$, which integrates the model E_A. We introduce the area term to avoid the non-manifoldness in the result. After obtained the new cost distributed graph $\mathcal{G}'$, the max-flow/min-cut algorithm is applied. The surface extracted from the min-cut would carry most of the features and is a close approximation to the minimum of $E_C(S)$. The reconstruction result of two cubes is shown in Figure 7(a).

It can be seen that most of edges and corners are fairly preserved. Ambiguous parts are only around the saddle points in Σ. In CAD examples, the obtained surface S' could be

TABLE 1
Graph Construction

Inputs	
1.	Graph $\mathcal{G}$ dual to the mesh
2.	$\mathcal{C}_+$, $\mathcal{C}_-$ as the min-cut of E_{V+} and E_{V-}
Algorithm	
1.	Initialize all $cost(n_i, n_j)$ by $d_{i,j}s_{i,j}$
2.	Initialize all $cost(s, n_i)$ and $cost(n_i, t)$ by a large value L
	%% Estimation from $\mathcal{C}_+$
3.	For each (n_i, n_j)
4.	If $(n_i, n_j) \in \mathcal{C}_+$, $n_i \in S$, $n_j \in T$
5.	calculate $\kappa_{i,j}$ from $\mathcal{C}_+$
6.	$cost(s, n_i) = \min\{\mu\kappa_{i,j}s_{i,j}/2, cost(s, n_i)\}$
7.	$cost(n_j, t) = \min\{\mu\kappa_{i,j}s_{i,j}/2, cost(n_j, t)\}$
8.	End If
9.	End For
	%% Similar procedure for $\mathcal{C}_-$
10.	$\vdots$
11.	Update $cost(n_i, n_j) = (d_{i,j} + \alpha)s_{i,j}$
Outputs	A new cost-distributed graph $\mathcal{G}'$

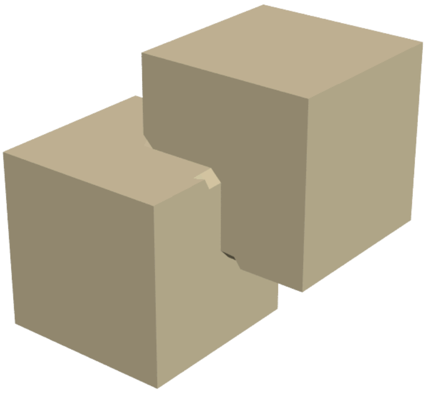

(a) Result from $\mathcal{G}'$

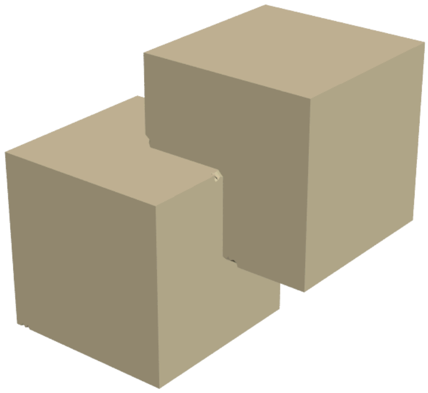

(b) Result for a higher resolution example

Fig. 7.

iteratively updated by the single swap further. In the examples where the features are not rigid, such as Happy Buddha and Dragon, S' is already a faithful enough reconstruction, which can be seen in Section 5. The whole pipeline of the reconstruction method described in this article can be visualized as the flowchart in Figure 8.

Compared with the previous iterative approach, the method proposed in this study has two advantages. (a) Efficiency. Most of features are recovered by a global approach by three graph-cuts instead of the local approach by iterative single swaps. In S', the ratio of unpreserved features to the whole amount is determined by the ratio of the saddle points to the whole feature points. Take the two cubes as example, this ratio is about $\frac{6}{350} \approx 0.017$. The low ratio suggests that the approximation S' is a quite faithful result. The workload for the subsequent local swap refinement is relatively small. Furthermore, in large scale example, this ratio would decrease further. See S' for a high resolution sample of two cubes in Figure 7(b). It is almost the original surface. (b) Robustness. The approximation obtained from three graph-cuts is already a surface close to the global minimum. The local minima trap in iteratively swapping approach can be avoided by choosing S' as a good initialization. In

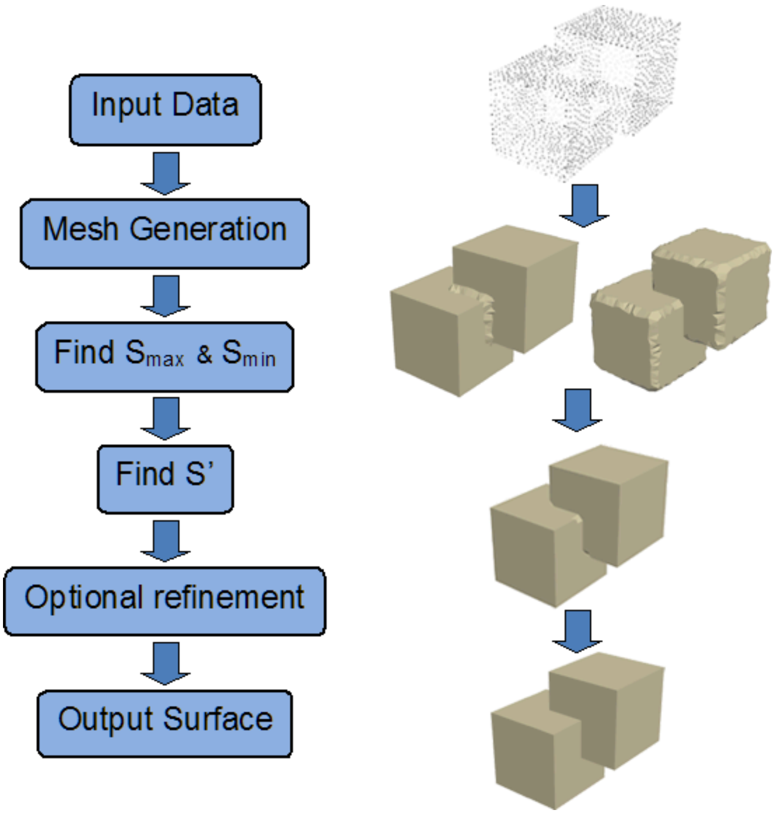

Fig. 8. Flowchart of the proposed method

summary, the method proposed in this study well solve the minimization with regard to curvature.

5 Numerical Examples

In this section, various numerical examples are provided to illustrate the effectiveness of the proposed method as well as the efficiency. All experiments had been conducted on a desktop PC with Intel Pentium 4 CPU of 3.2GHz. All CAD examples were synthesized by ourselves. Classic models were obtained from the Stanford 3D Scanning Repository (http://graphics.stanford.edu/data/3Dscanrep/) and Large Geometric Models Archive of Georgia Institute of Technology (http://www.cc.gatech.edu/projects/large_models/). Computational Geometry Algorithms Library [38] is used for mesh generation and the algorithm in [39] is used for graph-cuts. All reconstructed surfaces are rendered by PovRay [40]. Only points locations were utilized in the algorithm. All examples can be categorized into two groups: CAD examples and real examples.

In experiments, the curvature and area coefficients are chosen $\mu = 1$, $\alpha = 1$. To solve S_{min} and S_{max}, the coefficient β is selected according to Theorem 4. In practice, we choose $\beta = \frac{1}{3Volume(\Omega)} \cdot d(P,Q) \cdot s_\tau$.

CAD examples with rigid features, such as piecewise linear surface models, are presented in Figure 9. These examples include union, substraction, and intersection of basic geometries, which could well represent most models in various CAD applications. Input point sets, reconstruction surfaces, and the surface rendered according to the curvature are presented in columns. The curvature rendering highlights the feature.

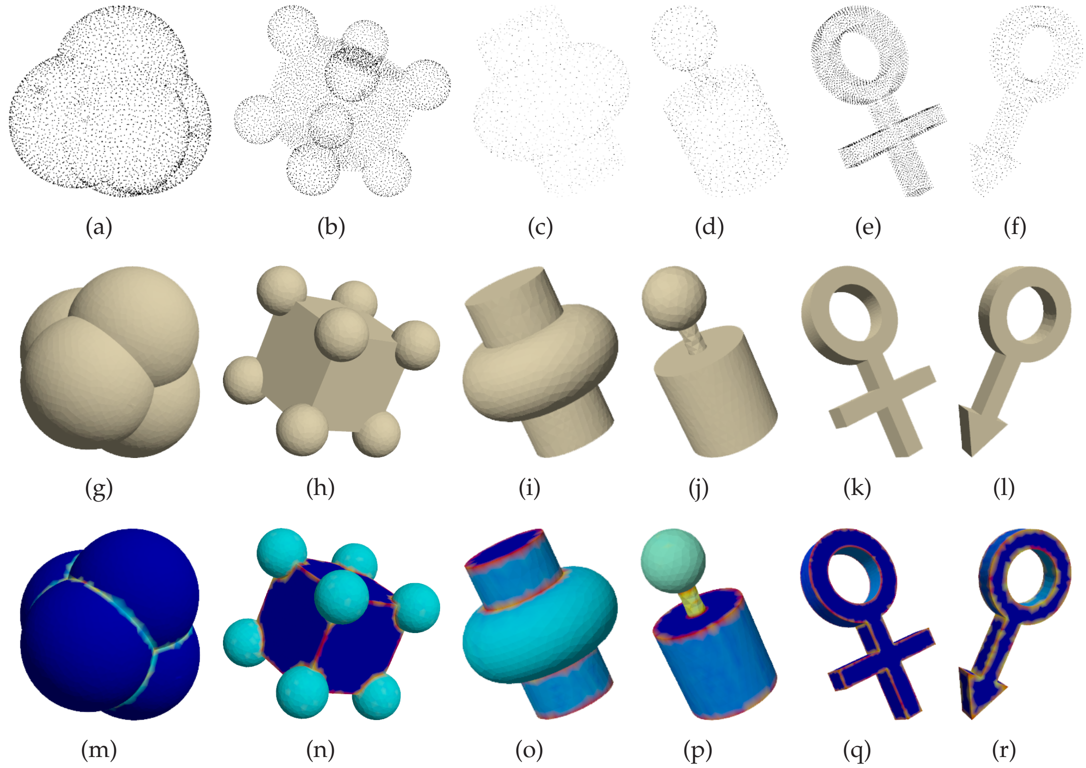

Fig. 9. CAD examples with rigid features: input data in the first row; reconstructed surface in the second row; curvature rendering surface in the third row.

All CAD results are the surfaces after iterative local swap refinement. This refinement workload is described in Section 4 and illustrated in Figure 7(b). Due to the rigid characteristic, the extra iterative refinement is necessary for CAD applications.

In Figure 11, all examples are scanned data from real models, such as the classic Happy Buddha and dragon. Reconstruction surfaces and the surface rendered according to the curvature are presented in columns. The global reconstruction result S' of these cases are presented instead of the result refined by iterative swaps. We can notice that these S' are so close an approximation that little difference could be told. In real applications, these results are satisfactory enough.

6 Conclusion

In this article, a surface reconstruction method with feature preservation is proposed based on Delaunay triangulation and graph-cuts. The proposed method could efficiently find a close approximation to the global minimum of a high order energy functional. Compared with the previous iterative approach, this close approximation could largely improve the efficiency and robustness.

Acknowledgments

This research is sponsored by Sinapore MOE ARC 29/07 T207B2202, MOE RG 59/08 M52110092, and NRF 2007IDM-IDM 002-010.

(a) (b) (c) (d)

Fig. 10. Examples of Happy Buddha and armadillo

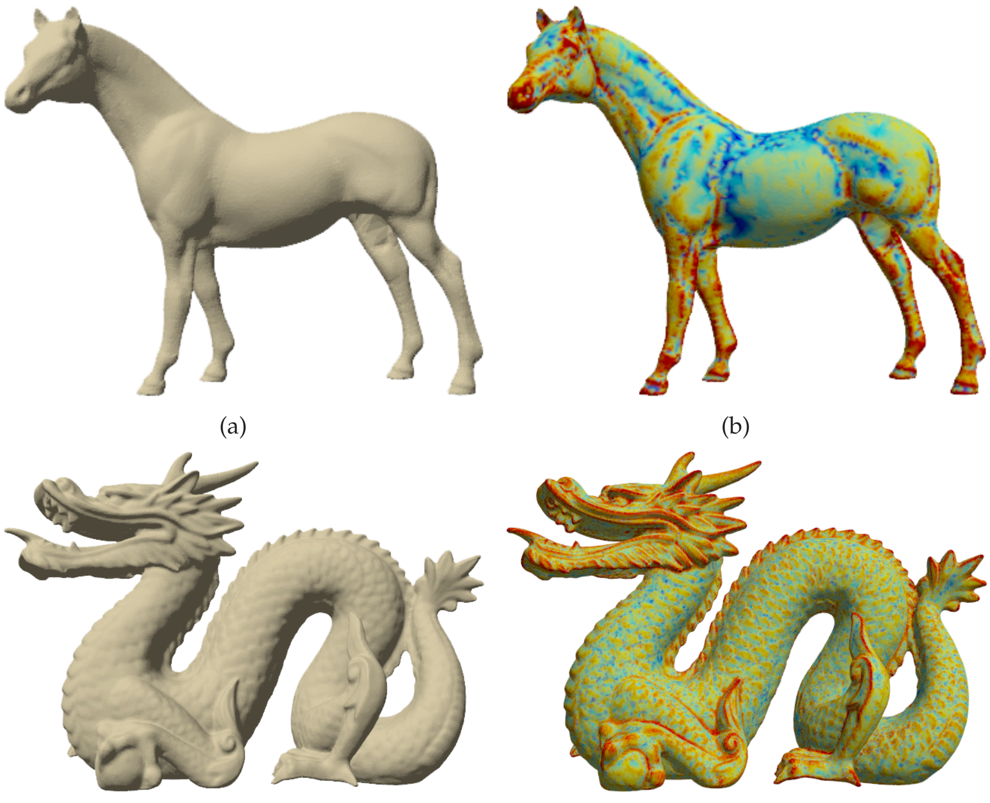

(a) (b)

(c) (d)

Fig. 11. Examples of horse and dragon.

REFERENCES

[1] N. Amenta, M. Bern, and M. Kamvysselis, "A new Voronoi-based surface reconstruction algorithm," in *Proceedings of the 25th annual conference on Computer graphics and interactive techniques*. ACM New York, NY, USA, 1998, pp. 415–421.

[2] H. Edelsbrunner and E. Mucke, "Three-dimensional alpha shapes," in *Proceedings of the 1992 workshop on Volume visualization*. ACM New York, NY, USA, 1992, pp. 75–82.

[3] F. Bernardini, J. Mittleman, H. Rushmeier, C. Silva, and G. Taubin, "The ball-pivoting algorithm for surface reconstruction," *Visualization and Computer Graphics, IEEE Transactions on*, vol. 5, no. 4, pp. 349–359, 1999.

[4] U. Adamy, J. Giesen, and M. John, "New techniques for topologically correct surface reconstruction," in *Proceedings of the conference on Visualization'00*. IEEE Computer Society Press Los Alamitos, CA, USA, 2000, pp. 373–380.

[5] T. K. Dey and S. Goswami, "Tight cocone: a water-tight surface reconstructor," in *SM '03: Proceedings of the eighth ACM symposium on Solid modeling and applications*, 2003, pp. 127–134.

[6] H. Hoppe, T. DeRose, T. Duchamp, J. McDonald, and W. Stuetzle, "Surface reconstruction from unorganized points," in *SIGGRAPH '92: Proceedings of the 19th annual conference on Computer graphics and interactive techniques*, 1992, pp. 71–78.

[7] M. Alexa, J. Behr, D. Cohen-Or, S. Fleishman, D. Levin, and C. Silva, "Point set surfaces," in *IEEE Visualization*, vol. 1, 2001, pp. 21–28.

[8] H. Zhao, S. Osher, and R. Fedkiw, "Fast surface reconstruction using the level set method," in *Proceedings of the IEEE Workshop on Variational and Level Set Methods (VLSM'01)*. IEEE Computer Society Washington, DC, USA, 2001, p. 194.

[9] E. Franchini, S. Morigi, and F. Sgallari, "Implicit shape reconstruction of unorganized points using PDE-based deformable 3D manifolds," *Numerical Mathematics: Theory, Methods and Applications*, 2010.

[10] E. Franchini, S. Morigi, and F. Sgallari, "Segmentation of 3D Tubular Structures by a PDE-Based Anisotropic Diffusion Model," *Mathematical Methods for Curves and Surfaces*, pp. 224–241, 2010.

[11] J. Barhak and A. Fischer, "Parameterization and reconstruction from 3d scattered points based on neural network and pde techniques," *Visualization and Computer Graphics, IEEE Transactions on*, vol. 7, no. 1, pp. 1–16, 2001.

[12] J. Solem and A. Heyden, "Reconstructing open surfaces from unorganized data points," in *IEEE Computer Society Conference on Computer Vision and Pattern Recognition*, vol. 2. IEEE Computer Society; 1999, 2004.

[13] A. Jalba and J. Roerdink, "Efficient surface reconstruction using generalized coulomb potentials," *Visualization and Computer Graphics, IEEE Transactions on*, vol. 13, no. 6, pp. 1512–1519, 2007.

[14] R. Paulsen, J. Baerentzen, and R. Larsen, "Markov random field surface reconstruction," *IEEE Transactions on Visualization and Computer Graphics*, pp. 636–646, 2009.

[15] K. Zhou, M. Gong, X. Huang, and B. Guo, "Data-parallel octrees for surface reconstruction," *IEEE Transactions on Visualization and Computer Graphics*, 2010.

[16] S. Corsaro, K. Mikula, A. Sarti, and F. Sgallari, "Semi-implicit covolume method in 3d image segmentation," *SIAM Journal on Scientific Computing*, vol. 28, no. 6, p. 2248, 2006.

[17] L. Evans and J. Spruck, "Motion of level sets by mean curvature i," *J. Diff. Geom*, vol. 33, no. 3, pp. 635–681, 1991.

[18] P. Perona and J. Malik, "Scale-space and edge detection using anisotropic diffusion," *Pattern Analysis and Machine Intelligence, IEEE Transactions on*, vol. 12, no. 7, pp. 629–639, 1990.

[19] A. Sarti, R. Malladi, and J. Sethian, "Subjective surfaces: a geometric model for boundary completion," *International Journal of Computer Vision*, vol. 46, no. 3, pp. 201–221, 2002.

[20] T. Tasdizen, R. Whitaker, P. Burchard, and S. Osher, "Geometric surface smoothing via anisotropic diffusion of normals," in *Visualization, 2002. VIS 2002. IEEE*. IEEE, 2002, pp. 125–132.

[21] M. Desbrun, M. Meyer, P. Schröder, and A. Barr, "Implicit fairing of irregular meshes using diffusion and curvature flow," in *Proceedings of the 26th annual conference on Computer graphics and interactive techniques*. ACM Press/Addison-Wesley Publishing Co., 1999, pp. 317–324.

[22] T. Goldstein, X. Bresson, and S. Osher, "Geometric applications of the split bregman method: Segmentation and surface reconstruction," *Journal of Scientific Computing*, vol. 45, no. 1, pp. 272–293, 2010.

[23] V. Boykov, "Computing geodesics and minimal surfaces via graph cuts," *Computer Vision, 2003. Proceedings. Ninth IEEE International Conference*, 2003.

[24] S. Paris, F. Sillion, and L. Quan, "A surface reconstruction method using global graph cut optimization," *International Journal of Computer Vision*, vol. 66, no. 2, pp. 141–161, 2006.

[25] Y. Boykov, O. Veksler, and R. Zabih, "Fast approximate energy minimization via graph cuts," *IEEE Transactions on Pattern Analysis and Machine Intelligence*, vol. 23, no. 11, pp. 1222–1239, 2001.

[26] V. Kolmogorov, R. Zabih, and S. Gortler, "Generalized multi-camera scene reconstruction using graph cuts," *Lecture notes in computer science*, pp. 501–516, 2003.

[27] M. Sormann, C. Zach, J. Bauer, K. Karner, and H. Bishof, "Watertight multi-view reconstruction based on volumetric graph-cuts," *Lecture Notes in Computer Science*, vol. 4522, p. 393, 2007.

[28] V. Kolmogorov and R. Zabin, "What energy functions can be minimized via graph cuts?" *IEEE Transactions on Pattern Analysis and Machine Intelligence*, vol. 26, no. 2, pp. 147–159, 2004.

[29] J. Shi, M. Wan, X. Tai, and D. Wang, "Curvature minimization for surface reconstruction with features," in *Third International Conference on Scale Space Methods and Variational Methods in Computer Vision,June 2011 Ein Gedi, Dead Sea, Israel*, 2011.

[30] T. Dey, *Curve and surface reconstruction: algorithms with mathematical analysis*. Cambridge Univ Pr, 2007, pp. 6–7.

[31] M. Wan, Y. Wang, and D. Wang, "Variational surface reconstruction based on Delaunay triangulation and graph cut," *International Journal for Numerical Methods in Engineering*, vol. 85, no. 2, pp. 206–229, 2011.

[32] M. Wan, Y. Wang, E. Bae, X.-C. Tai, and D. Wang, "Reconstructing open surfaces via graph-cuts," *IEEE Transactions on Visualization and Computer Graphics*, vol. 99, no. PrePrints, 2012.

[33] M. Meyer, M. Desbrun, P. Schröder, and A. Barr, "Discrete differential-geometry operators for triangulated 2-manifolds," *Visualization and mathematics*, vol. 3, no. 7, pp. 34–57, 2002.

[34] G. Xu, "Discrete laplace-beltrami operators and their convergence," *Computer Aided Geometric Design*, vol. 21, no. 8, pp. 767–784, 2004.

[35] R. Garimella and B. Swartz, "Curvature estimation for unstructured triangulations of surfaces," *Los Alamos National Laboratory*, 2003.

[36] A. McIvor and R. Valkenburg, "A comparison of local surface geometry estimation methods," *Machine Vision and Applications*, vol. 10, no. 1, pp. 17–26, 1997.

[37] S. Petitjean, "A survey of methods for recovering quadrics in triangle meshes," *ACM Computing Surveys (CSUR)*, vol. 34, no. 2, pp. 211–262, 2002.

[38] "Cgal, Computational Geometry Algorithms Library," 1997, http://www.cgal.org.

[39] Y. Boykov and V. Kolmogorov, "An experimental comparison of min-cut/max-flow algorithms for energy minimization in vision," *IEEE Transactions on Pattern Analysis and Machine Intelligence*, pp. 1124–1137, 2004.

[40] "Pov–team, persistence of vision raytracer (povray)," 2004, http://www.povray.org.